Novel Boxlike Dinuclear or Chain Polymeric Silver(I) Complexes with Polypyridyl Bridging Ligands: Syntheses, Crystal Structures, and Spectroscopic and Electrochemical Properties

Xian-He Bu,* He Liu, and Miao Du

Department of Chemistry, Nankai University, Tianjin 300071, P. R. China

Keith Man-Chung Wong and Vivian Wing-Wah Yam*

Department of Chemistry, The University of Hong Kong, Pokfulam Road, Hong Kong, P. R. China

Mitsuhiko Shionoya

Department of Chemistry, Graduate School of Science, The University of Tokyo, Hongo, Tokyo, Japan

Received January 11, 2001

The syntheses, characterization, crystal structures, and photophysical and electrochemical properties of two dinuclear and two polymeric Ag^I complexes with three polypyridyl ligands, 2,3-di-2-pyridylquinoxaline (**L**$^{\mathbf{1}}$), 2,3-di-2-pyridyl-5,8-dimethoxyquinoxaline (**L**$^{\mathbf{2}}$), and 2,3,7,8-tetrakis(2-pyridyl)pyrazino[2,3-*g*] quinoxaline (**L**$^{\mathbf{3}}$), are described. The structures of the two boxlike dinuclear complexes with **L**$^{\mathbf{1}}$ and **L**$^{\mathbf{2}}$ and two chemically the same but differently crystallized one-dimensional zigzag chain coordination polymers also consisting of boxlike dinuclear subunits have been elucidated by X-ray analysis. $[Ag\mathbf{L}^{\mathbf{1}}(CH_3CN)]_2$-$(BF_4)_2 \cdot 2CHCl_3$ (**1**): monoclinic, *C*2/*c*; a = 28.631(2), b = 12.2259(11), c = 14.3058(12) Å; β = 99.180(2)°; Z = 4. $[Ag\mathbf{L}^{\mathbf{2}}(CH_3CN)_2]_2(ClO_4)_2$ (**2**): triclinic, $P\bar{1}$; a = 12.3398(2), b = 13.750(2), c = 14.326(7) Å; α = 83.494(3), β = 74.631(3), γ = 76.422(3)°; Z = 4. $\{[Ag_2\mathbf{L}^{\mathbf{3}}(NO_3)_2] \cdot CH_3CN\}_\infty$ (**3a**): monoclinic, $P2_1/c$; a = 9.5836(8), b = 13.4691(12), c = 14.0423(12) Å; β = 107.753(2)°; Z = 4. $[Ag_2\mathbf{L}^{\mathbf{3}}(NO_3)_2]_\infty$ (**3b**): monoclinic, $P2_1/c$; a = 8.4689(6), b = 16.0447(12), c = 11.7307(8) Å; β = 102.051(1)°; Z = 2. The structures of the dinuclear complexes **1** and **2** are similar to each other, with the two intramolecular Ag^I centers of each complex being spanned by two ligands thus forming a unique boxlike cyclic dimer. In **1**, each Ag^I center is four-coordinated by three nitrogen atoms of two **L**$^{\mathbf{1}}$ ligands and a CH_3CN nitrogen donor, taking a distorted tetrahedral coordination geometry. The coordination environment of Ag^I in **2** is similar to that in **1**, except the formation of an additional weak coordination bond with the oxygen atom of the methoxy group of **L**$^{\mathbf{2}}$. The structures of **3a,b** are very similar to each other, except for the stacking patterns in the crystal lattices, and the cyclic boxlike dinuclear unit, which is similar to the structure of **1**, constitutes the fundamental building block to form the one-dimensional zigzag chain structures due to the "end-on" nature of **L**$^{\mathbf{3}}$. **1**−**3** exhibit metal-perturbed intraligand transitions in solution in 360−390 nm regions. Cyclic voltammetric studies of these complexes show the presence of reduction peak at ∼−0.5 V vs $Fc^{+/0}$. In the solid state at 77 K, they exhibit broad emission that may be assignable to originate from the metal-perturbed intraligand transitions.

Introduction

The transition metal complexes with polypyridyl bridging ligands are of considerable interest because of their potential as building blocks for supramolecular assemblies and their photophysical and redox properties, which make them useful as light-harvesting complexes and photonic molecular devices[1−3] and particularly desirable for solar energy conversion schemes.[4] The metal complexes of 2,3-di-2-pyridylquinoxaline and its analogue have been extensively studied, where the metal centers are mainly Ru^{II}, Os^{II}, and Re^I.[5−7] The photophysical and spectroelectrochemical properties of d^{10} transition metal (e.g., Cu^I, Ag^I, Au^I) complexes with such ligands are topics of developing interest.[8] The d^{10} configuration of the metal center and the π^* orbitals of the ligand centers are combined to produce low-lying metal-to-ligand charge-transfer (MLCT) and intraligand (IL) transitions, which significantly affect the emission behaviors of these systems. So far, such studies have been mostly confined to the Cu^I and Au^I complexes,[9] while the Ag^I complexes are relatively less explored compared to those of its congeners despite the remarkably rich and well-known photochemistry of Ag^I halides.[10,11]

* Corresponding authors. E-mail for X.-H.B.: buxh@nankai.edu.cn. Fax for X.-H.B.: ++86-22-23530850.

(1) For examples, see: (a) Fujita, M.; Oguro, D.; Miyazawa, M.; Oka, H.; Yamaguchi, K.; Ogura, K. *Nature* **1995**, *378*, 469. (b) Hannon, M. J.; Painting, C. L.; Errington, W. *Chem. Commun.* **1997**, 1805. (c) Withersby, M. A.; Blake, A. J.; Champness, N. R.; Hubberstey, P.; Li, W. S.; Schröder, M. *Angew. Chem., Int. Ed. Engl.* **1997**, *36*, 2327. (d) Balzani, V.; Campagana, S.; Denti, G.; Juris, A.; Serroni, S.; Venturi, M. *Acc. Chem. Res.* **1998**, *31*, 26. (e) Ibukuro, F.; Kusukawa, T.; Fujita, M. *J. Am. Chem. Soc.* **1998**, *120*, 8561. (f) Blake, A. J.; Champness, N. R.; Hubberstey, P.; Li, W. S.; Withersby, M. A.; Schröder, M. *Coord. Chem. Rev.* **1999**, *183*, 117. (g) Hagrman, P. J.; Hagrman, D.; Zubieta, J. *Angew. Chem., Int. Ed. Engl.* **1999**, *38*, 2638. (h) Umemoto, K.; Yamaguchi, K.; Fujita, M. *J. Am. Chem. Soc.* **2000**, *122*, 7150. (i) Leininger, S.; Olenyuk, B.; Stang, P. J. *Chem. Rev.* **2000**, *100*, 853. (j) Bu, X. H.; Morishta, H.; Tanaka, K.; Biradha, K.; Furusho, S.; Shionoya, M. *Chem. Commun.* **2000**, 971. (k) Bu, X. H.; Biradha, K.; Yamaguchi, T.; Nishimura, M.; Ito, T.; Tanaka, K.; Shionoya, M. *Chem. Commun*. **2000**, 1953.

10.1021/ic010044o CCC: $20.00
Published on Web 07/14/2001

Incorporating a ligand with two chelating sites into the coordination sphere allows systematic construction of large supramolecular assemblies, capable of acting as antennae in the energy conversion schemes,[12] where the photochemical and redox properties of the complexes are strongly dependent on the nature of the ligands.[13] The addition of different groups alters the electronic energy of the π-accepting properties of the bridging ligand, since the π-accepting molecular orbital is the important factor in controlling the extent of the metal−metal communication in these polynuclear systems.[14] In our effort to study the metal complexes of polypyridyl ligands, we report herein the syntheses of two dinuclear Ag^{I} complexes with 2,3-di-2-pyridylquinoxaline (**L**^{1}) and 2,3-di-2-pyridyl-5,6-dimethoxylquinoxaline (**L**^{2}) and two chemically the same but differently crystallized one-dimensional zigzag chain Ag^{I} coordination polymers with 2,3,7,8-tetrakis(2-pyridyl)pyrazino[2,3-*g*]quinoxaline (**L**^{3}) (see Chart 1). The structures and luminescence and electrochemical properties of these complexes have been studied in detail.

Chart 1

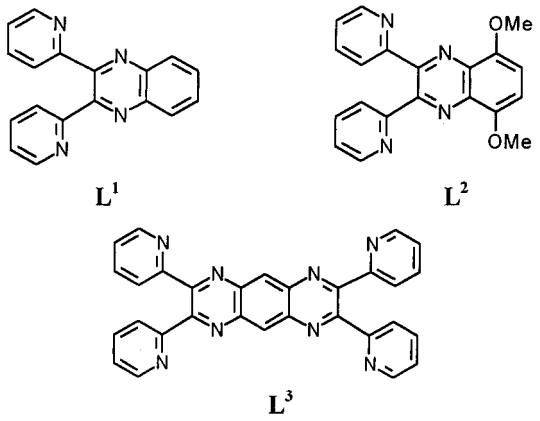

L^{1} **L**^{2} **L**^{3}

Experimental Section

Materials and General Methods. All the reagents for syntheses were commercially available and used without further purification or purified by standard methods prior to use. Elemental analyses were performed on a Perkin-Elmer 240C analyzer. IR spectra were measured on a FT-IR 170SX (Nicolet) spectrometer with KBr pellets and electronic spectra on a Hitachi UV-3010 spectrometer. ^{1}H NMR spectra were recorded on a Bruker AC-P500 spectrometer (500 MHz) at 25 °C in $CDCl_3$ with tetramethylsilane as the internal reference. The ESI mass spectra were recorded on a TSQ 7000 triple-quadrupole tandom mass spectrometer (Finnigan MAT) with Finnigan ESI-Intreface. Data recording and evaluation were carried out using the ICIS 8.1 software package (Finnigan MAT).

Photochemistry. Steady-state excitation and emission spectra were obtained on a Spex Fluorolog 111 spectrafluorometer equipped with a Hamamatsu R-928 photomultiplier tube. Low-temperature (77 K) spectra were recorded by using an optical Dewar sample holder. Emission lifetime measurements were performed using a conventional laser system, and the excitation source was a 355 nm output (third harmonic) of Quanta-Ray Q-switched GCR-150 pulsed Nd:YAG laser (10 Hz).

Electrochemistry. Cyclic voltammograms (CV) were obtained by a CH Instruments Inc. CHI 620 electrochemical analyzer equipped with a glassy-carbon electrode as a working electrode, a $Ag/AgNO_3$ electrode (0.1 mol dm^{-3} in CH_3CN) as a reference electrode, and a platinum electrode as an auxiliary electrode, respectively. Solutions of complexes **1**−**3** (0.1 mmol dm^{-3}) were prepared by dissolving the appropriate amount of the complex in rigorously dried acetonitrile with 0.1 mol dm^{-3} n-Bu_4NPF_6 ($(TBA)PF_6$) as the supporting electrolyte. The tested systems were purged with argon for ca. 20 min prior to recording the CV trace at 298 K. The cyclic voltammograms were recorded at a scan rate of 100 mV^{-1}.

Syntheses of Ligands. 2,3-Di-2-pyridylquinoxaline (L^{1}) and 2,3,7,8-tetrakis(2-pyridyl)pyrazino[2,3-g]quinoxaline (L^{3}) were synthesized and purified according to the literature methods[15,16] by the reaction of corresponding *o*-diamines (*o*-phenyldiamine or 1,2,4,5-benzenetetramine) and 2,2′-pyridil.

2,3-Di-2-pyridyl-5,8-dimethoxyquinoxaline (L^{2}). 1,4-Dimethoxy-2,3-dinitrobenzene and 1,4-dimethoxy-2,3-phenylenediamine were synthesized according to the literature methods.[17] A solution of newly prepared 1,4-dimethoxy-2,3-phenylenediamine (0.4 g, 2.38 mmol) in ethanol (10 mL) was added to a solution of 2,2′-pyridil (0.5 g, 2.38 mmol) in ethanol (20 mL) under argon, and the mixture was heated at reflux for 4 h (Scheme 1). Upon cooling, the light yellow cubic crystals of **L**^{2} were separated and recrystallized twice from CH_3OH/CH_2Cl_2

(2) For examples, see: (a) Balzani, V.; Juris, M.; Venturi, M.; Campagna, S.; Serrioni, S. *Chem. Rev.* **1996**, *96*, 759. (b) Bignozzi, C. A.; Schoonover, J. R.; Scandola, F. *Prog. Inorg. Chem*. **1997**, *44*, 1. (c) Moser, J. E.; Bonnote, P.; Grätzel, M. *Coord. Chem. Rev*. **1998**, *177*, 245. (d) Balzani, V.; Gómez-López, M.; Stoddart, J. F. *Acc. Chem. Res.* **1998**, *31*, 405.

(3) For examples, see: (a) Eggleston, M. K.; McMillin, D. R.; Koenig, K. S.; Pallenberg, A. J. *Inorg. Chem.* **1997**, *36*, 172. (b) Ziessel, R.; Harriman, A. *Coord. Chem. Rev.* **1998**, *171*, 331. (c) Venturi, M.; Serroni, S.; Juris, A.; Campagna, S.; Balzani, V. *Top. Curr. Chem.* **1998**, *197*, 193. (d) Miller, M. T.; Gantzel, P. K.; Karpishin, T. B. *J. Am. Chem. Soc.* **1999**, *121*, 4292.

(4) (a) Nazeeruddin, M. K.; Kay, A.; Rodicio, I.; Humphry-Baker, R.; Müller, E.; Liska, P.; Vlachopoulos, N.; Grätzel, M. *J. Am. Chem. Soc.* **1993**, *115*, 6382. (b) Kalyanasundaram, K.; Grätzel, M. *Coord. Chem. Rev*. **1998**, *177*, 347.

(5) (a) Wallace, A. W.; Murphy, W. R., Jr.; Petersen, J. D. *Inorg. Chim. Acta* **1989**, *166*, 47. (b) Ruminski, R. R.; Deere, P. T.; Oliver, M.; Serveiss, D. *Inorg. Chim. Acta* **1998**, *281*, 1. (c) Scott, S. M.; Gordon, K. C.; Burrell, A. K. *J. Chem. Soc., Dalton Trans.* **1999**, 2669.

(6) (a) Richter, M. M.; Brewer, K. J. *Inorg. Chem*. **1993**, *32*, 5762. (b) Ruminski, R. R.; Serveiss, D.; Jacquez, M. *Inorg. Chem.* **1995**, *34*, 3358. (c) Grosshenny, V.; Harriman, A.; Ziessel, R. *Angew. Chem., Int. Ed. Engl.* **1995**, *34*, 1100. (d) Brewer, K. J. *Comments Inorg. Chem.* **1999**, *21*, 201.

(7) (a) Kalyanasundaram, K.; Nazeeruddin, M. K. *J. Chem. Soc., Dalton Trans.* **1990**, 1657. (b) Ruminski, R. R.; Lehmpuhl, D. *Inorg. Chim. Acta* **1993**, *204*, 45. (c) Waterland, M. R.; Simpson, T. J.; Gordon, K. C.; Burrell, A. K. *J. Chem. Soc., Dalton Trans.* **1998**, 185.

(8) (a) Crosby, G. A.; Highland, R. G.; Truesdell, K. A. *Coord. Chem. Rev.* **1985**, *64*, 41. (b) Kutal, C. *Coord. Chem. Rev.* **1990**, *99*, 213. (c) Miller, M. T.; Gantzel, P. K.; Karpishin, T. B. *Angew. Chem., Int. Ed. Engl.* **1998**, *37*, 1556.

(9) (a) McMillin, D. R.; Kirchoff, J. R.; Goodwin, K. V. *Coord. Chem. Rev*. **1985**, *64*, 831. (b)Yam, V. W. W.; Lo, K. K. W. *J. Chem. Soc., Dalton Trans.* **1995**, 499. (b) Gordon, K. C.; Al-Obaidi, A. H. R.; Jayaweera, P. M.; McGarvey, J. J.; Malone, J. F.; Bell, S. E. J. *J. Chem. Soc., Dalton Trans*. **1996**, 1591. (c) Tang, S. S.; Chang, C. P.; Lin, I. J. B.; Liou, L. S. *Inorg. Chem*. **1997**, *36*, 2294. (d) Pyykkö, P. *Chem. Rev.* **1997**, *97*, 597. (e) Yam, V. W. W.; Lo, K. K. W. *Comments Inorg. Chem.* **1997**, *19*, 209. (f) Mansour, M. A.; Connick, W. B.; Lachicotte, R. J.; Gysling, H. J.; Einsenberg, R. *J. Am. Chem. Soc.* **1998**, *120*, 1329. (g) Miller, M. T.; Gantzel, P. K.; Karpishin, T. B. *Inorg. Chem*. **1999**, *38*, 3414.

(10) (a) Che, C. M.; Yip, H. K.; Yam, V. W. W.; Cheung, P. Y.; Lai, T. F.; Shieh, S. J.; Peng, S. M. *J. Chem. Soc., Dalton Trans*. **1992**, 427. (b) Yam, V. W. W.; Lo, K. K. W.; Wang, C. R.; Cheung, K. K. *Inorg. Chem*. **1996**, *35*, 5116. (c) Yam, V. W. W.; Chong, S. H. F.; Wong, K. M. C.; Cheung, K. K. *Chem. Commun.* **1999**, 1013.

(11) (a) Vogler, A.; Kunkely, H. *Chem. Phys. Lett.* **1989**, *158*, 74. (b) Vogler, A.; Quett, C.; Kunkely, H. *Ber. Bunsen-Ges. Phys. Chem.* **1988**, *92*, 1486. (c) Sabin, F.; Ryu, C. K.; Ford, P. C.; Vogler, A. *Inorg. Chem*. **1992**, *31*, 1941.

(12) (a) DeCola, L.; Belser, P. *Coord. Chem. Rev*. **1998**, *177*, 301. (b) Ward, M. D.; White, C. M.; Barigelletti, F.; Armaroli, N.; Calogero, G.; Flamigni, L. *Coord. Chem. Rev.* **1998**, *171*, 481.

(13) (a) Ziessel, R.; Hissler, M.; El-Ghayoury, A.; Harriman, A. *Coord. Chem. Rev*. **1998**, *180*, 1251. (b) Waterland, M. R.; Flood, A.; Gordon, K. C. *J. Chem. Soc., Dalton Trans*. **2000**, 121.

(14) (a) Callahan, R. W.; Brown, G. M.; Meyer, T. J. *Inorg. Chem.* **1975**, *14*, 1443. (b) Creutz, C. *Prog. Inorg. Chem.* **1983**, *30*, 1.

(15) Goodwin, H. A.; Lions, F. *J. Am. Chem. Soc.* **1959**, *81*, 6415.

(16) Rillema, D. P.; Mack, K. B. *Inorg. Chem.* **1982**, *21*, 3849.

Scheme 1

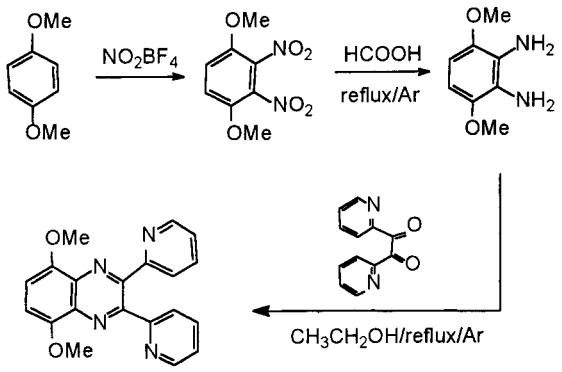

(yield: 0.74 g, 90%). Mp: 230−231 °C. ^{1}H NMR ($CDCl_3$): δ 4.07 (s, 6H), 7.07 (s, 2H), 7.19−7.21 (m, 2H). 7.74−7.81 (m, 2H), 8.03 (m, 2H), 8.32 (d, 2H, J = 4.2 Hz). Anal. Calcd for $C_{20}H_{16}N_4O_2$: C, 69.75; H, 4.68; N, 16.27. Found: C, 70.15; H, 4.84; N, 16.05. IR (KBr pellet, cm^{-1}): 1611 m, 1587 m, 1466 m, 1173 m, 1357 m, 1333 m, 1279 s, 1253 w, 1135 m, 1111 s.

Caution! While we have met no problems in handling perchlorate salts through this work, these should be treated with great caution due to their potential explosive nature.

Syntheses of the Ag^I Complexes. [Ag(L^1)(CH$_3$CN)]$_2$[BF$_4$]$_2$·2CHCl$_3$ (1). A solution of $AgBF_4$ (20 mg, 0.1 mmol) in CH_3CN (5 mL) was added to a stirred solution of **L^1** (28 mg, 0.1 mmol) in $CHCl_3$ (10 mL) at room temperature, giving a yellow solution immediately. The reaction mixture was stirred for ca. 1 h and then filtered. The filtrate was kept to stand in the dark, and after ca. 1 week, red cubic single crystals suitable for X-ray analysis were obtained. Yield: 45 mg (70%). IR (KBr pellet, cm^{-1}): 2919 w, 2253 w, 1630 w, 1589 m, 1481 m, 1352 m, 1083 s, 1076 s, 789 m, 747 s, 548 w. Positive ESI-MS: ion cluster at m/z 869 {[Ag$_2$(**L^1**)$_2$(BF$_4$)]$^+$} and 675 {[Ag(**L^1**)$_2$]$^+$}. Anal. Calcd for $C_{42}H_{32}Ag_2N_{10}B_2F_8Cl_6$: C, 39.45; H, 2.52; N, 10.95. Found: C, 39.21; H, 2.59; N, 10.88.

[Ag(L^2)(CH$_3$CN)]$_2$(ClO$_4$)$_2$ (2). Complex **2** was prepared by a procedure similar to that of **1**. A mixture of $AgClO_4$·$6H_2O$ (47 mg, 0.15 mmol) in CH_3CN (5 mL) and **L^2** (52 mg, 0.15 mmol) in $CHCl_3$ (10 mL) was stirred for ca. 30 min and then filtered. After ca. 1 week, the solution afforded red single crystals suitable for X-ray analysis. Yield: 75 mg (85%). IR (KBr pellet, cm^{-1}): 2247 m, 1606 m, 1595 m, 1494 s, 1352 m, 1280 s, 1173 m, 1102 s, 665 m, 622 s. Positive ESI-MS: ion cluster at m/z 1003 {[Ag$_2$(**L^2**)$_2$(ClO$_4$)]$^+$} and 797 {[Ag(**L^2**)$_2$]$^+$}. Anal. Calcd for $C_{44}H_{38}Ag_2N_{10}O_{12}Cl_2$: C, 44.58; H, 3.23; N, 11.82. Found: C, 44.21; H, 3.39; N, 11.60.

{[Ag$_2$(L^3)(NO$_3$)$_2$]·CH$_3$CN}$_\infty$ (3a) and [Ag$_2$(L^3)(NO$_3$)$_2$]$_\infty$ (3b). Layering a solution of $AgNO_3$ (34 mg, 0.2 mmol) in CH_3CN (5 mL) upon a solution of **L^3** (49 mg, 0.1 mmol) in $CHCl_3$ (10 mL) in a sealed tube with very careful and subsequent diffusion. After several days, yellow cubic crystals of **3a** together with a few orange red crystals of **3b** suitable for X-ray analysis were adhering to the wall of the tube. The mixture complexes were separated under the microscope by a tweezer. **3a** was the main product. Yield: 64 mg (70%). IR (KBr pellet, cm^{-1}): 3058 w, 2247 w, 1587 m, 1566 m, 1471 m, 1384 s, 1038 s, 778 s. Positive ESI-MS: ion cluster at m/z 1429 {[Ag$_3$(**L^3**)$_2$(NO$_3$)$_2$]$^+$}, 1258 {[Ag$_2$(**L^3**)$_2$(NO$_3$)]$^+$}, and 1089 {[Ag(**L^3**)$_2$]$^+$}, respectively. Anal. Calcd for $C_{34}H_{24}Ag_2N_{12}O_6$: C, 44.76; H, 2.65; N, 18.42. Found: C, 44.64; H, 2.71; N, 18.39. **3b** was obtained only in ca. 1% yield. Anal. Calcd for $C_{30}H_{18}Ag_2N_{10}O_6$: C, 43.40; H, 2.19; N, 16.87. Found: C, 43.22; H, 2.31; N, 16.66.

Crystallographic Studies. Single-crystal X-ray diffraction measurements were carried out with a Bruker Smart 1000 CCD at 293 ± 2 K (for **1** and **3a,b**) and at 193 ± 2 K (for **2**). Each diffractometer was equipped with a graphite crystal monochromator situated in the incident beam for data collection. The determination of unit cell parameters and data collections were performed with Mo Kα radiation (λ = 0.710 73 Å). Unit cell dimensions were obtained with least-squares refinements, and all the structures were solved by direct methods. Ag^I atoms in each complex were located from *E*-maps. The other non-hydrogen atoms were located in successive difference Fourier syntheses. The final refinement was performed by full-matrix least-squares methods with anisotropic thermal parameters for non-hydrogen atoms on F^2. The hydrogen atoms were added theoretically, riding on the concerned atoms and refined with fixed thermal factors. Crystallographic data and experimental details for structural analyses are summarized in Table 1.

Results and Discussion

Syntheses and General Characterization. The polypyridyl bridging ligands **L^1** and **L^3** were prepared in high yields by literature methods.[15−17] Several steps, as depicted in Scheme 1, are required for the preparation of the new ligand **L^2**. The intermediate, 1,4-dimethoxy-2,3-phenylenediamine, was not stable in air, and it was used directly in the next condensation reaction without purification. **L^2** was obtained in a high yield and could be easily purified by recrystallization from MeOH and CH_2Cl_2. The spectral and elemental analysis data are satisfactory as required for these compounds.

Because of the light-sensitive nature of the Ag^I complexes, all the preparations were carried out in the dark or protected from light by aluminum foil at room temperature. Single crystals of **1** and **2** suitable for X-ray analysis could be obtained directly from the reaction mixture in high yield, while those of **3a,b** were obtained by diffusion method. The spectral and elemental analysis data are also satisfactory as required for these compounds.

Description of the Crystal Structures. Dinuclear Complex 1. An ORTEP view of **1** including the atomic numbering scheme is shown in Figure 1a, and the selected bond distances and angles are given in Table 2. The structure consists of two Ag^I centers related by a C_2 symmetry and spanned by two **L^1** ligands to form a unique boxlike cyclic dimeric structure. Each Ag^I center is four-coordinated to form a distorted tetrahedral geometry with two nitrogen donors, one from the pyrazine ring and one from a pyridine ring of one **L^1** ligand, and a nitrogen atom of the pyridine ring from another **L^1** ligand, as well as the nitrogen atom of an acetonitrile molecule. The interesting feature of this structure is the formation of the discrete boxlike dimer in which two of the potentially tetradentate **L^1** ligands jointly coordinate to the Ag^I centers by using three nitrogen atoms of each ligand and by rotating the pyridyl rings out of the plane of the quinoxaline system. Such a coordination mode prevents the formation of infinite end-on structures. This is a new coordination mode for **L^1**, of which the usual symmetric coordination mode is to form dinuclear metal complexes as has been found for some complexes of this ligand.[4c,9b] As shown in Figure 1b, the distance between parallel neighboring aromatic rings in the dimer is ca. 3.34 Å, indicating the presence of significant face-to-face $\pi-\pi$ stacking,[18] and this strong interaction might be a driving force for the formation of this dimeric structure. In addition, the distance between the intermolecular adjacent aromatic rings is ca. 3.55 Å, the intra- and intermolecular face-to-face aryl interactions link the complexes into an infinite quasi-one-dimension chain, and this may stabilize the complex in the crystal.

(17) (a) Dwyer, C. L.; Holzapfel, C. W. *Tetrahedron* **1998**, *54*, 7843. (b) Shaikh, I. A.; Johnson, F.; Grollman, A. P. *J. Med. Chem.* **1986**, *29*, 1329. (c) Entwistle, I. D.; Jackson, A. E.; Johnstone, A. W.; Telford, R. P. *J. Chem. Soc., Perkin Trans. 1* **1977**, 443.

(18) (a) Hunter, C. A.; Sanders, J. K. M. *J. Am. Chem. Soc.* **1990**, *112*, 5525. (b) Sauvage, J. P.; Collin, J. P.; Chambron, J. C.; Guillerez, S.; Coudret, C. *Chem. Rev.* **1994**, *94*, 993. (c) Desiraju, G. R. *Chem. Commun.* **1997**, 1475.

Table 1. Crystallographic Data and Structural Refinement Summary for **1**, **2**, **and 3a,b**

	1	**2**	**3a**	**3b**
formula	$C_{42}H_{32}Ag_2Cl_6B_2F_8N_{10}$	$C_{44}H_{38}Ag_2Cl_2N_{10}O_{12}$	$C_{34}H_{24}Ag_2N_{12}O_6$	$C_{30}H_{18}Ag_2N_{10}O_6$
M_r	1278.84	1185.48	912.40	830.28
space group	*C*2/*c*	$P\bar{1}$	$P2_1/c$	$P2_1/c$
T (K)	298 ± 2	193 ± 2	298 ± 2	298 ± 2
a (Å)	28.631(2)	12.3398(2)	9.5836(8)	8.4689(6)
b (Å)	12.2259(11)	13.750(2)	13.4691(12)	16.0447(12)
c (Å)	14.3058(12)	14.326(7)	14.0423(12)	11.7307(8)
α (deg)	90	83.494(3)	90	90
β (deg)	99.180(2)	74.631(3)	107.753(2)	102.051(1)
γ (deg)	90	76.422(3)	90	90
V (Å^3)	4943.5(7)	2275.0(6)	1726.3(3)	1558.85(19)
ρ_{calcd} (g cm^{-3})	1.718	1.731	1.676	1.769
Z	4	4	4	2
μ (cm^{-1})	11.90	10.54	12.00	13.17
R	0.0452	0.0519	0.0351	0.0324
R_w	0.1317	0.1071	0.0868	0.0949

The Ag−N bond distances vary from 2.232(4) to 2.507(7) Å, all being within the normal range observed in the polypyridyl Ag^I complexes.[19] The Ag−$N_{pyrazine}$ bond distances are considerably longer than the Ag−$N_{pyridine}$ lengths by 0.13 and 0.20 Å due to the weaker *σ*-donor strength of the pyrazine group[20] and steric crowding.[21] The Ag(1) ion deviates ca. 0.52 Å from the plane defined by N(5), N(1), and N(2), and the angles of N(5)−Ag(1)−N(1), N(1)−Ag(1)−N(2), and N(2)−Ag(1)−N(5) are 148.46(17), 71.03(19), and 118.88(18)°, respectively. These values and the longer distance of Ag(1)−N(4) (2.507(7) Å) suggest that the Ag^I ion is in a distorted tetrahedral environment. The intramolecular Ag(1)···Ag(1A) nonbonding distance is 4.638 Å. The shortest Ag···F separation between the Ag^I center and BF_4^- anion is 2.969 Å, suggesting a very weak interaction.

L^1 splays the two pyridyl rings apart with respect to the quinoxaline ring, which is nonplanar with the pyrazine ring showing a slight twist conformation with respect to the benzo moiety (a 3.2° dihedral angle). Comparing the structure of **1** to the free ligand **L^1**,[21] we can find that the free ligand has both pyridine nitrogens rotated toward the center; however, in **1**, each **L^1** splays one pyridine ring to coordinate to another metal center. Furthermore, in **1**, the dihedral angles between the two pyridyl groups and the quinoxaline and the two pyridyl groups in each ligand are 54.0, 30.7, and 49.2°, respectively. One might have expected that the coordinated pyridine ring would lie in the same plane with the coordinated pyrazine ring; this is not the case as suggested by the dihedral angle mentioned above. The rotating of the pyridine rings out of the plane of the quinoxaline system removes some steric crowding and takes advantage of coordinating with another Ag^I atom to form a dinuclear unit.

Dinuclear Complex 2. The ORTEP structure of the dimeric complex $[Ag(\mathbf{L^2})(CH_3CN)]_2 \cdot 2ClO_4$ (**2**) is shown in Figure 2a, and the relevant bond distances and angles are listed in Table 3. The structure is very similar to that of **1**. Each Ag^I center is also coordinated with three nitrogen atoms of two **L^2** ligands and a nitrogen atom of an acetonitrile. The two Ag^I centers have pseudo-C_2 symmetrical relationship. The Ag−N bond distances vary from 2.196(6) to 2.466(8) Å, all being within the normal range observed in polypyridyl Ag^I complexes.[19] The Ag−$N_{pyrazine}$ bond distances are also considerably longer than those of the Ag−$N_{pyridine}$ bonds by 0.15−0.21 Å. The distances between the Ag^I centers and the nearer O atoms of the methoxyl groups [Ag(1)−O(22B), 2.756 Å; Ag(2)−O(21A), 2.882 Å] indicate the existence of weak interactions. The Ag(1) and Ag(2) centers reside ca. 0.49 and 0.42 Å outward from the planes defined by [N(41A), N(12B), and N(41B)] and [N(11A), N(31A), and N(31B)], respectively. The intramolecular nonbonding distance of Ag(1)···Ag(2) is 4.575 Å, slightly shorter than that in **1**, probably due to a weak coordination of the $-OCH_3$ groups in **2**. The dihedral angles between the two pyridyl rings and the quinoxaline and the two pyridyl rings are 55.5, 29.7, and 47.9°, respectively, which are also slightly different from those in **1**. As shown in Figure 2b, the distance between parallel neighboring aromatic rings in the dimer is ca. 3.49 Å, also slightly shorter than that in **1**, indicating the presence of stronger face-to-face *π*−*π* stacking. In a way similar to that for complex **1**, the distance between the intermolecularly adjacent aromatic rings is ca. 3.44 Å in the crystal packing of complex **2**, and an infinite quasi-one-dimensional chain is also formed by the inter- and intramolecular face-to-face aryl interactions such as **1**. In a word, the two $-OCH_3$ groups of **L^2** increased the electron density of the quinoxaline ring, improved its *π*-electron-donating ability, and resulted in different emission properties of the two complexes which will be discussed later in this paper.

Polymeric Chain Complexes 3a,b. As **L^3** can be considered as a fused compound of two **L^1** groups in an "end-to-end" fashion, it may coordinate to metal ions in an "end-on" mode to form a zigzag infinite one-dimensional chain complex. This is confirmed by the formation of two similar polymeric Ag^I complexes **3a,b**. The coordination geometries of Ag^I in **3a,b** are quite similar, only differing in the packing modes in their crystals. There are noncoordinated acetonitrile molecules in the crystal lattice of **3a**, whereas, there are no such acetonitrile molecules in **3b** (see Figure 4). Such a different packing pattern between the two crystals led to a slight differences of the bond distances and angles in the two complexes.

The ORTEP view of a dinuclear segment of the infinite chain structure of **3a** (**3b** is similar to **3a**) is shown in Figure 3, and the selected bond distances and angles are listed in Table 4. The coordination mode of half of the **L^3** ligand is quite similar to that of **L^1**, except that the nitrate ions take the place of the acetonitrile ligand in complexes **3a,b**. Each Ag^I center is four-coordinated with three nitrogen atoms of two **L^3** ligands and

(19) (a) Pallenberg, A. J.; Marschner, T. M.; Barnhart, D. M. *Polyhedron* **1997**, *16*, 2771. (b) Kaes, C.; Hosseini, M. W.; Rickard, C. E. F.; Skelton, B. W.; White, A. H. *Angew. Chem., Int. Ed. Engl.* **1998**, *37*, 920.

(20) (a) Rillema, D. P.; Taghdiri. D. G.; Jones, D. S.; Keller, C. D.; Worl, L. A.; Meyer, T. J.; Levy, H. A. *Inorg. Chem.* **1987**, *26*, 578. (b) Escuer, A.; Vicenta, R.; Comas, T.; Ribas, J.; Gomez, M.; Solans, X.; Gatteschi, D.; Zanchini, C. *Inorg. Chim. Acta* **1991**, *181*, 51.

(21) Rasmussen, S. C.; Richer, M. M.; Yi, E.; Place, H.; Brewer, K. J. *Inorg. Chem.* **1990**, *29*, 3926.

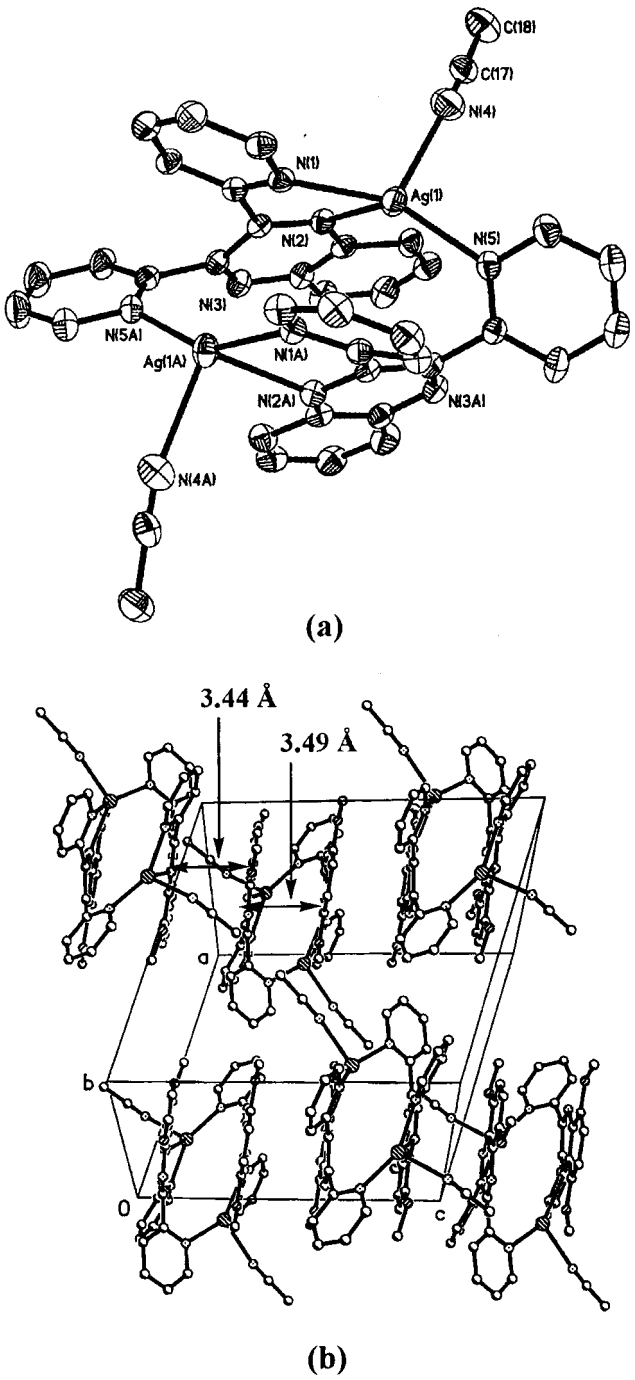

Figure 1. (a) ORTEP view of the complex cation of **1** with 30% thermal ellipsoid probability. (b) Packing diagram in the unit cell showing the boxlike cavity of each molecule and the inter- and intramolecular $\pi-\pi$ stacking.

Table 2. Selected Bond Lengths (Å) and Angles (deg) for **1**

Bond Lengths (Å)			
Ag(1)−N(5)	2.232(4)	Ag(1)−N(1)	2.271(5)
Ag(1)−N(2)	2.432(5)	Ag(1)−N(4)	2.507(7)
Ag(1)···F(1)	2.969	Ag(1)···Ag(2)	4.638
Bond Angles (deg)			
N(5)−Ag(1)−N(1)	148.46(17)	N(5)−Ag(1)−N(2)	118.88(18)
N(1)−Ag(1)−N(2)	71.03(19)	N(5)−Ag(1)−N(4)	97.99(19)
N(1)−Ag(1)−N(4)	112.29(19)	N(2)−Ag(1)−N(4)	90.7(2)

one oxygen donor of a NO_3^- anion (not acetonitrile). In **3a**, the $Ag-N_{pyrazine}$ bond distances are considerably longer than the $Ag-N_{pyridine}$ bond lengths by 0.15 and 0.17 Å. However,

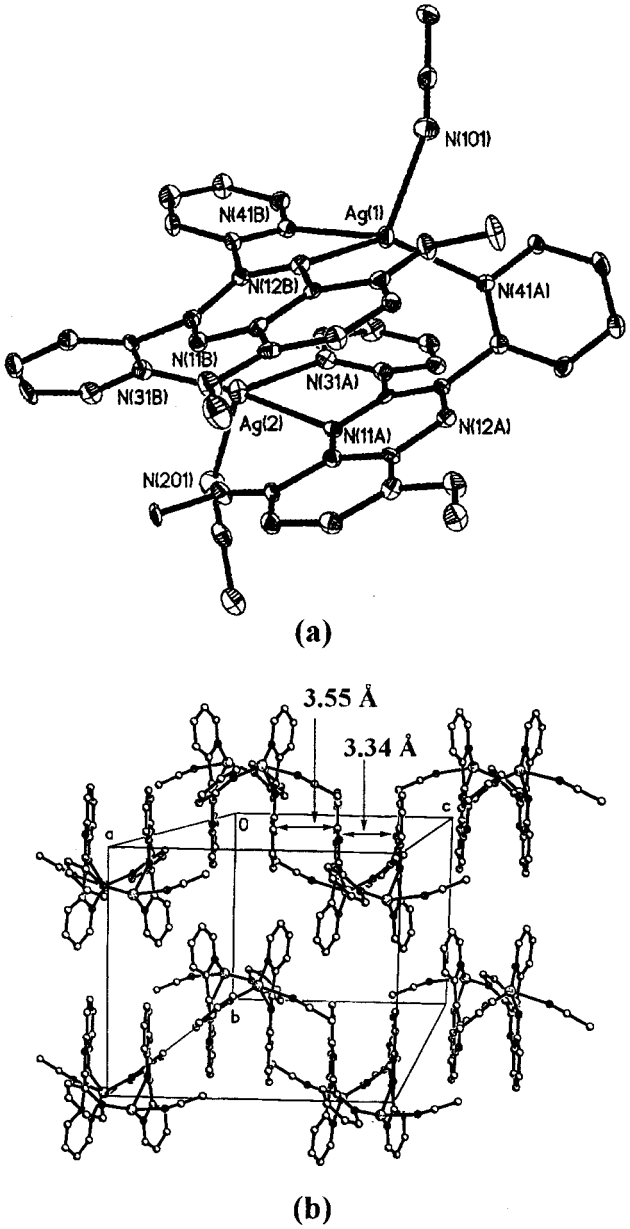

Figure 2. (a) ORTEP view of the complex cation of **2** with 30% thermal ellipsoid probability. (b) Packing diagram in the unit cell showing the boxlike cavity of each molecule.

Table 3. Selected Bond Lengths (Å) and Angles (deg) for **2**

Bond Lengths (Å)			
Ag(1)−N(12B)	2.425(6)	Ag(1)−N(41B)	2.275(6)
Ag(1)−N(41A)	2.270(6)	Ag(1)−N(101)	2.402(8)
Ag(2)−N(31B)	2.196(6)	Ag(2)−N(31A)	2.250(7)
Ag(2)−N(11A)	2.460(6)	Ag(2)−N(201)	2.466(8)
Ag(1)−O(22B)	2.756	Ag(2)−O(21A)	2.882
Ag(1)···Ag(2)	4.575		
Bond Angles (deg)			
N(12B)−Ag(1)−N(41A)	125.4(2)	N(41A)−Ag(1)−N(41B)	146.3(2)
N(12B)−Ag(1)−N(41B)	70.2(2)	N(41A)−Ag(1)−N(101)	94.0(2)
N(12B)−Ag(1)−N(101)	123.0(3)	N(41B)−Ag(1)−N(101)	100.5(3)
N(31B)−Ag(2)−N(31A)	149.9(2)	N(11A)−Ag(2)−N(31B)	125.1(2)
N(31A)−Ag(2)−N(41B)	70.3(3)	N(31B)−Ag(2)−N(201)	100.4(2)
N(31A)−Ag(2)−N(201)	100.2(3)	N(11A)−Ag(2)−N(201)	103.4(2)

in **3b** the $Ag-N_{pyridine}$ bond distance is 0.11 Å longer than the $Ag-N_{pyrazine}$ bond. In **3a**, the Ag^I center resides ca. 0.43 Å (0.63 Å for **3b**) from the plane defined by N(1), N(2), and N(3), and the sum of the three angles N(1)−Ag(1)−N(2),

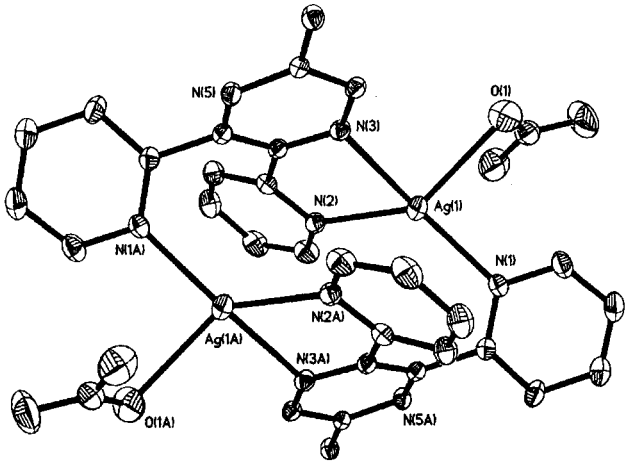

Figure 3. ORTEP view of a binuclear box segment of **3a** with 30% thermal ellipsoid probability.

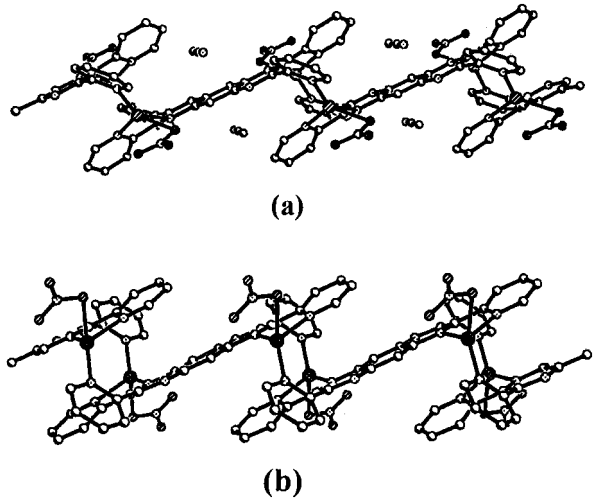

Figure 4. One-dimensional zigzag chain structures of (a) **3a** and (b) **3b.**

Table 4. Selected Bond Lengths (Å) and Angles (deg) for **3a,b**

param	3a	3b
Bond Lengths (Å)		
Ag(1)−N(1)	2.275(4)	2.224(3)
Ag(1)−N(2)	2.305(4)	2.341(3)
Ag(1)−N(3)	2.450(3)	2.320(3)
Ag(1)−O(1A)	2.596(4)	2.461(4)
Ag(1)···Ag(1A)	4.626	5.018
Bond Angles (deg)		
N(1)−Ag(1)−N(2)	127.33(13)	130.62(11)
N(1)−Ag(1)−N(3)	148.12(12)	133.38(10)
N(2)−Ag(1)−N(3)	70.79(12)	69.54(10)
N(1)−Ag(1)−O(1)	89.93(14)	105.63(12)
N(2)−Ag(1)−O(1)	134.91(15)	90.56(12)
N(3)−Ag(1)−O(1)	90.72(12)	116.74(12)

N(1)−Ag(1)−N(3), and N(2)−Ag(1)−N(3) is 346.2° (333.5° for **3b**), suggesting that the Ag^I ion is in a distorted tetrahedral coordination geometry in **3a,b**. The intramolecular nonbonding Ag(1)···Ag(1a) distance is 4.626 Å (5.018 Å for **3b**).

The dihedral angles between the two pyridyl groups, the quinoxaline, and the two pyridyl groups are 62.5, 19.4, and 62.5° for **3a**, respectively (54.1, 38.0, and 50.3°, respectively, for **3b**).

Electronic Spectra and Electrochemical Properties. The electronic absorption, luminescence, and electrochemical data for **1**−**3a** are summarized in Table 5. The electronic absorption spectra of **1**−**3a**, obtained in CH_3CN for **1** and **2** and in DMF for **3a**, display intense absorption bands associated with the metal-perturbed IL (intraligand) transitions and IL (intraligand) transitions in the range of 200−500 nm. **1** and **2** display shoulder absorption bands due to the metal-perturbed IL (intraligand) transitions, probably with some metal-to-ligand charge-transfer character, 361 and 391 nm, respectively, while complex **3a** displays an intense absorption at 398 nm. In addition, the spectral region between ca. 200 to 330 nm contains broad intense absorptions which are mainly ligand-centered $\pi \rightarrow \pi^*$ transitions.

Cyclic voltammetric studies of **1**−**3** in CH_3CN solution (**3a,b** are the same in CH_3CN solution) with 0.1 mol dm^{-3} *n*-Bu_4NPF_6 as supporting electrolyte showed that each complex displays an irreversible reduction wave at ca. −0.5 V vs $Fc^{+/0}$. In addition, quasi-reversible reduction couples were observed at ca. −1.9 V vs $Fc^{+/0}$ for **1** and **2**, while two quasi-reversible reduction couples were observed at ca. −1.2 and −1.8 V vs $Fc^{+/0}$ for **3** (Figure 5). The resemblance of the potentials for the irreversible reduction wave at ca. −0.5 V vs. $Fc^{+/0}$, which is different from a related Cu^I complex, $[Cu\mathbf{L^2}(CH_3CN)]_2 \cdot 2ClO_4$ (E_{pc} = −0.973 V vs $Fc^{+/0}$),[22] is suggestive of its origin as a Ag^I metal-centered reduction. On the other hand, the quasi-reversible reduction couples at ca. −1.9 to −2.0 V vs. $Fc^{+/0}$ in **1** and **2** as well as those at ca. −1.2 and −1.8 V in **3** are assigned as the polypyridyl ligand-centered reductions. The more negative $E_{1/2}$ value in **2** than that in **1** is in accordance with the reduced ease of reduction of $\mathbf{L^2}$ relative to $\mathbf{L^1}$ in the presence of the electron-donating methoxyl substituents. The less negative $E_{1/2}$ values for the reduction of **3** than those of **1** and **2** are also consistent with the increased ease of reduction of $\mathbf{L^3}$ as a consequence of its better π-accepting ability resulting from an increase in its extended π-conjugation. The oxidation of **1** occurred at +1.273 V vs $Fc^{+/0}$ with an irreversible wave. Studies of **2** and **3** showed the presence of quasi-reversible oxidation couples at +1.014 and +1.330 V vs $Fc^{+/0}$, respectively. The relatively greater ease of oxidation of **2** than that of **1** and **3,** as well as the well-known difficulty in Ag^I oxidation, suggested that the oxidation processes are likely to be ligand-centered in nature rather than metal-centered. This has further been supported by the close resemblance of the $E_{1/2}$ values between **2** and its related Cu^I analogue, $[Cu\mathbf{L^2}(CH_3CN)]_2 \cdot 2ClO_4$ ($E_{1/2}$ = +1.033 V vs $Fc^{+/0}$).[22]

Luminescence Studies. The luminescence behaviors of **1**−**3a** have been studied both at 298 and 77 K. Complexes **1** and **3a** were found to be weakly luminescent to almost nonemissive at 298 K in the solid state, while **2** exhibited a broad, structureless emission spectrum maximizing at 605 nm with a lifetime less than 0.1 μs in the solid state. At 77 K, the emission maxima of **1** and **2** were at ca. 585 and 598 nm, respectively, in the solid state (Figure 6) and appeared to be vibronically structureless, while **3a** did not show any emission upon excitation at λ = 380 nm, with only a high-energy emission band at 410 nm observed upon high-energy UV excitation. The spectra of **1** and **2** dissolved in a frozen MeOH/EtOH glass (1:4 v/v) at 77 K reveal the emission maxima at 524 and 518 nm, respectively; the emission band of **1** is vibronically structured with vibrational progressional spacings of ca. 1200 cm^{-1} typical of aromatic ring deformation modes of the polypyridyl ligands. Unlike the related Cu^I polypyridyl systems,[9a,b] the transitions associated with the emissions at ca. 520−600 nm in **1** and **2** are believed to originate predominantly from a metal-perturbed IL excited state, while the high-energy emission at 410 nm in **3a**, which

(22) Bu, X. H.; Liu, H.; Du. M.; Yam, V. W.-W. Unpublished results.

Table 5. Spectroscopic and Electrochemical Data for **1**−**3a**

	abs,[a] λ_{max}/nm	emission[b]		$E_{1/2}$/V (ΔE_p/mV)[c]	
complex	($10^{-3}\epsilon_{max}$/dm^3 mol^{-1} cm^{-1})	medium (T/K)	λ_{max}/nm	oxidn	redn
1	361 (0.7, sh)	solid (298)	nonemissive	+1.273[d]	−0.535[e]
	331 (11.9)	solid (77)	585		−1.939 (86)
	264 (24.5)	EtOH/MeOH (77)	524		
	244 (42.5)				
	227 (34.1)				
2	391 (2.9, sh)	solid (298)	605 (<0.1 μs)	+1.014 (75)	−0.533[d]
	286.5 (53.2)	solid (77)	598		−1.998 (70)
	197 (45.1)	EtOH/MeOH (77)	518		
3a	398 (9.9)	solid (298)	nonemissive	+1.33 (97)	−0.499[d]
	293 (22.0)	solid (77)	410		−1.267 (60)
	268 (21.3)	EtOH/MeOH (77)	nonemissive		−1.802 (67)

[a] 0.1 mmol dm^{-3} in CH_3CN or DMF solution (the formulas used to calculate the ϵ values were as follows: $C_{42}H_{32}Ag_2Cl_6B_2F_8N_{10}$ for **1**, $C_{44}H_{38}Ag_2Cl_2N_{10}O_{12}$ for **2,** and $C_{34}H_{24}Ag_2N_{12}O_6$ for **3a**). [b] λ_{em} = 380 nm. [c] In CH_3CN (0.1 mol dm^{-3} *n*-Bu_4NPF_4); potentials/V vs $F_c^{+/0}$ (ΔE_p ($F_c^{+/0}$) ~ 65−70 mV); scan rate = 100 mV/s. [d] E_{pa} value. [e] E_{pc} value.

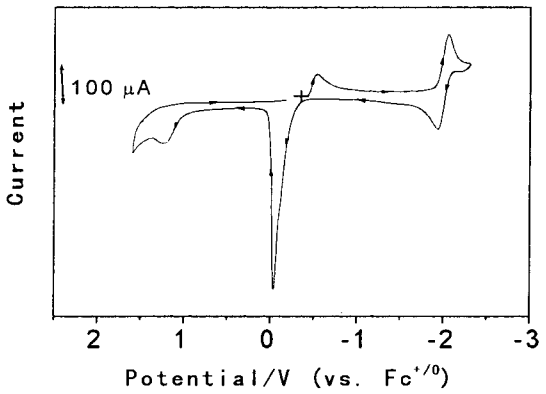

Figure 5. Cyclic voltammograms for **1** in 0.1 mol dm^{-3} (TBA)PF_6 acetonitrile solution.

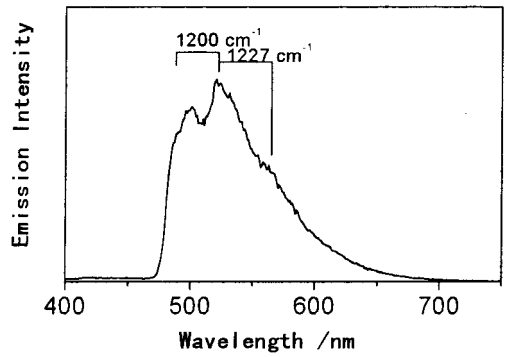

Figure 6. Emission spectrum of **1** in the glass state (4:1 EtOH/MeOH) at 77 K.

occurs only with high-energy excitation, is mainly IL $\pi \rightarrow \pi^*$ transition in character.

Conclusion and Comments

Two boxlike dinuclear (**1** and **2**) and two polymeric one-dimensional zigzag chain (**3a,b**) Ag^I complexes have been prepared with a series of polypyridyl ligands: 2,3-di-2-pyridylquinoxaline ($\mathbf{L^1}$), 2,3-di-2-pyridyl-5,6-dimethoxylquinoxaline ($\mathbf{L^2}$), and 2,3,7,8-tetrakis(2-pyridyl)pyrazino[2,3-*g*]quinoxaline ($\mathbf{L^3}$). The crystal structures, luminescence, and electrochemical properties of **1**, **2**, and **3a** have been studied. All the Ag^I centers in the four complexes are four-coordinated, and two metal centers are bridged by two ligands forming the unique cyclic boxlike dimeric structure units. This is a new coordination mode for such polypyridyl ligands. The zigzag chain polymeric complexes **3a,b** are formed by the replication of the cyclic dimeric unit with the two terminal of $\mathbf{L^3}$ which can be considered a fused compound of two $\mathbf{L^1}$ units in an "end-to-end" fashion. In this dinuclear system of **1** and **2**, the inter- and intramolecular face-to-face aryl interactions between parallel neighboring aromatic rings form a quasi-one-dimensional chain, and this stabilizes the whole structure of the two complexes. Cyclic voltammetric studies show that all the complexes display an irreversible Ag^I metal-centered reduction wave. All the complexes are emissive in the solid state and frozen alcohol glass originated from metal-perturbed IL or pure IL excited state. **1** and **2** exhibit emission spectra in the solid state and frozen alcohol glass at low temperature assigned to the metal-perturbed excited state. **3** is found to be very weakly luminescent and only emits in the solid state. Only **2** exhibits emission spectra in the solid state at 298 K, indicating the effect of the electron-donating methoxy group on $\mathbf{L^2}$.

Acknowledgment. This work was financially supported by the National Natural Science Foundation of China (No. 29971019) and the Trans-Century Talents Training Program Foundation from the State Education Ministry of China. We thank Dr. Biradha Kumar for the analysis of the structure of complex **2**.

Supporting Information Available: Tables of complete X-ray data and X-ray crystallographic files in CIF format for the structure determinations of **1**−**3b**. This material is available free of charge via the Internet at http://pubs.acs.org.

IC010044O